

Contents lists available at [SciVerse ScienceDirect](http://SciVerse.ScienceDirect.com)

Biochimica et Biophysica Acta

journal homepage: www.elsevier.com/locate/bbabio

Defective mitochondrial translation differently affects the live cell dynamics of complex I subunits

Cindy E.J. Dieteren^{a,b}, Peter H.G.M. Willems^a, Herman G. Swarts^a, Jack Fransen^{c,d}, Jan A.M. Smeitink^b, Werner J.H. Koopman^{a,*}, Leo G.J. Nijtmans^b

^a Department of Biochemistry, Nijmegen Centre for Molecular Life Sciences, Radboud University Nijmegen Medical Centre, PO Box 9101, 6500 HB, Nijmegen, The Netherlands

^b Department of Pediatrics, Laboratory of Pediatrics and Neurology, Nijmegen Center for Mitochondrial Disorders, Radboud University Nijmegen Medical Centre, PO Box 9101, 6500 HB, Nijmegen, The Netherlands

^c Department of Cell Biology, Nijmegen Centre for Molecular Life Sciences, Radboud University Nijmegen Medical Centre, PO Box 9101, 6500 HB, Nijmegen, The Netherlands

^d Microscopic Imaging Centre, Nijmegen Centre for Molecular Life Sciences, Radboud University Nijmegen Medical Centre, PO Box 9101, 6500 HB, Nijmegen, The Netherlands

ARTICLE INFO

Article history:

Received 14 July 2011

Received in revised form 16 September 2011

Accepted 18 September 2011

Available online 24 September 2011

Keywords:

Doxycycline

Mitochondria

FRAP

AcGFP1

Fluorescence gel analysis

Chloramphenicol

ABSTRACT

Complex I (CI) of the oxidative phosphorylation system is assembled from 45 subunits encoded by both the mitochondrial and nuclear DNA. Defective mitochondrial translation is a major cause of mitochondrial disorders and proper understanding of its mechanisms and consequences is fundamental to rational treatment design. Here, we used a live cell approach to assess its consequences on CI assembly. The approach consisted of fluorescence recovery after photobleaching (FRAP) imaging of the effect of mitochondrial translation inhibition by chloramphenicol (CAP) on the dynamics of AcGFP1-tagged CI subunits NDUFV1, NDUFS3, NDUFA2 and NDUFB6 and assembly factor NDUF4. CAP increased the mobile fraction of the subunits, but not NDUF4, and decreased the amount of CI, demonstrating that CI is relatively immobile and does not associate with NDUF4. CAP increased the recovery kinetics of NDUFV1-AcGFP1 to the same value as obtained with AcGFP1 alone, indicative of the removal of unbound NDUFV1 from the mitochondrial matrix. Conversely, CAP decreased the mobility of NDUFS3-AcGFP1 and, to a lesser extent, NDUFB6-AcGFP1, suggestive of their enrichment in less mobile subassemblies. Little, if any, change in mobility of NDUFA2-AcGFP1 could be detected, suggesting that the dynamics of this accessory subunit of the matrix arm remains unaltered. Finally, CAP increased the mobility of NDUF4-AcGFP1, indicative of interaction with a more mobile membrane-bound subassembly. Our results show that the protein interactions of CI subunits and assembly factors are differently altered when mitochondrial translation is defective.

© 2011 Elsevier B.V. All rights reserved.

1. Introduction

Complex I (CI) is one of the five multi-subunit enzymes of the mitochondrial oxidative phosphorylation (OXPHOS) system. The enzyme exhibits several functions including the oxidation of NADH, reduction of ubiquinone, conveyance of electrons released at the site of NADH oxidation to the site of ubiquinone reduction and utilization of part of their redox energy to transfer protons across the mitochondrial inner membrane (MIM). As such, CI plays a crucial

role in the conversion of redox energy into the electrochemical proton gradient used by complex V to synthesize ATP.

Human CI is built from 45 different proteins with an estimated size of 1 MDa. The complex has an L-shaped structure with a peripheral arm protruding in the matrix and a MIM-embedded membrane arm. Functionally, CI can be divided into a dehydrogenase module, which oxidizes NADH, a hydrogenase module, which transfers the electrons and has been suggested to operate as a redox-driven proton pump, and a transporter module, proposed to act as a conformation-driven proton pump [15]. According to a hypothetical scheme of the evolution of CI, the dehydrogenase module is thought to consist of at least the NDUFV1, NDUFV2 and NDUFS1 subunits, the hydrogenase module of at least the NDUFS2, NDUFS3, NDUFS7, NDUFS8, ND1 and ND5 subunits and the transporter module of at least the ND2, ND3, ND4, ND4L, and ND6 subunits [16]. The 7 ND subunits are encoded by the mitochondrial genome (mtDNA), whereas the 7 NDUF subunits are encoded by the nuclear DNA (nDNA). In mammals, the nDNA also encodes another 31 supernumerary or accessory subunits, whose function is only beginning to be understood.

Abbreviations: AcGFP1, *Aequorea coerulescens* green fluorescent protein; BN-PAGE, blue native polyacrylamide gel electrophoresis; CAP, chloramphenicol; CI, complex I; F_m , mobile fraction; FRAP, fluorescence recovery after photobleaching; MIM, mitochondrial inner membrane; MtDNA, mitochondrial DNA; MW, molecular weight; nDNA, nuclear DNA; NDUF, NADH dehydrogenase ubiquinone flavoprotein

* Corresponding author at: Department of Biochemistry (286), Nijmegen Centre for Molecular Life Sciences (NCMLS), Radboud University Nijmegen Medical Centre (RUNMC), P.O. Box 9101, NL-6500 HB Nijmegen, The Netherlands. Tel.: +31 24 3614589; fax: +31 24 3616413.

E-mail address: w.koopman@ncmls.ru.nl (W.J.H. Koopman).

Emerging evidence supports the concept that CI assembly is a multi-step process, in which several subunits are first combined into smaller intermediates of the three functional modules. Subsequently, the holo-enzyme is formed by joining these preassembled modules and additional subunits [2,11,22,27,40,41,44]. Parallel to this *de novo* assembly route, an 'exchange pathway' was proposed, in which newly imported subunits replace their previously incorporated counterparts in the holo enzyme. This mechanism might serve to restore oxidatively damaged CI subunits [22]. Several non-structural proteins have been identified to be required for proper assembly of CI [1,7,12,13,23–25,30,31,34,39,42,43]. Recent blue native electrophoresis work revealed that two of these assembly factors, NDUFAF3 and NDUFAF4, are present in several NDUF3-containing subcomplexes [31]. It was proposed that NDUFAF4 forms a MIM-associated complex with an early peripheral arm assembly intermediate and NDUFAF3 bound to the mitochondrial assembly machinery. In this way, NDUFAF3 assists in MIM insertion of newly formed ND subunits, thus allowing their joining with the early CI assembly intermediate.

Together, these findings indicate that CI assembly is a highly dynamic process warranting detailed investigation in live cells. To this end we stably expressed six AcGFP1-tagged CI subunits in HEK293 cells [11]. Using fluorescence recovery after photobleaching (FRAP) analysis, we provided evidence that each subunit was partially present in holo CI. Four subunits (NDUFV1, NDUFV2, NDUF2, and NDUF12) were also present as highly mobile matrix-soluble monomers, whereas two other subunits (NDUFB6 and NDUF3) were additionally present in a slowly mobile fraction. In the case of the integral MIM protein NDUFB6, this fraction most likely represents one or more membrane-bound subassemblies, whereas biochemical evidence suggests that for the NDUF3 protein this fraction might correspond to a matrix-soluble subassembly [11].

Maintenance of cellular CI levels requires the biosynthesis of not only its mtDNA- and nDNA-encoded structural subunits along with its nDNA-encoded assembly factors but also of nDNA-encoded constituents of the mitochondrial import machinery and nDNA-encoded factors controlling the stability, replication, transcription and translation of the mtDNA [21]. Malfunction of CI can be caused by defects at each of these levels as has been demonstrated in patients with isolated or combined CI deficiency [36]. Defective mitochondrial translation leads to a marked reduction in CI expression [8,35]. However, so far no live cell information is available on the effect of this condition on the dynamics of the CI assembly process. Therefore, we here performed FRAP analysis on cells expressing the AcGFP1-tagged versions of the nDNA-encoded structural subunits NDUFV1, NDUF3 and NDUFB6, predicted to be part of the dehydrogenase, hydrogenase and membrane module, respectively. In addition, we included accessory subunit NDUF2, located in the matrix-protruding arm of CI, and CI assembly factor NDUFAF4. Mutations in both proteins have been identified in patients with CI deficiency, demonstrating their essential role in CI maintenance [20,31].

Our results reveal that CI structural proteins and assembly factors display different live cell dynamics upon depletion of mtDNA-encoded (ND) subunits, which may be indicative of the relative stabilities of the corresponding functional modules and/or their intermediates.

2. Materials and methods

2.1. Cell lines and cell culture

Cell lines expressing AcGFP1-tagged versions of NDUFV1, NDUF3, NDUF2, NDUFB6 and NDUFAF4 and control cell lines expressing matrix-targeted AcGFP1 (GFP), the matrix-targeted tandem version of AcGFP1 (GFP²) and AcGFP1-tagged ANT1 were generated as described previously [10,11]. Cells were cultured in DMEM (Biowhitaker, Walkersville, MD, USA) supplemented with 10% (v/v) fetal calf serum,

1% penicillin/streptomycin (Gibco, Breda, The Netherlands), 200 µg/ml hygromycin (Calbiochem, Brunschwig, Amsterdam, The Netherlands) and 50 µg/ml blasticidin (Invitrogen, Breda, The Netherlands). All cell lines, except those expressing the tagged versions of NDUFB6, GFP² and ANT, displayed low steady-state expression levels already in the absence of doxycycline. Therefore, expression of NDUFB6, GFP² and ANT was induced by adding 1 µg/ml of doxycycline (Sigma, Zwijndrecht, The Netherlands) to the medium during the last 24 h of culture. Mitochondrial translation was inhibited by adding 40 µg/ml of chloramphenicol (CAP; Sigma) to the medium for 3 days prior to harvesting of the cells for PAGE analysis or FRAP imaging.

2.2. BN-PAGE and SDS-PAGE analysis

After harvesting of the cells, mitochondrial lysates were prepared and run on native 5–15% gradient gels as described previously [6]. In-gel fluorescence emission was scanned using an imaging analyzer (FLA5000, Fujifilm, Tilburg, The Netherlands) equipped with a 473 nm excitation laser and a FITC filter (>510 nm). Subsequently, duplo gels were stained for CI in-gel activity as described in [6] or blotted on nitrocellulose using an iBlot® Dry Blotting System (Invitrogen) after 10 min incubation with 2× Nu-PAGE transfer buffer (Invitrogen). A separate fraction of mitochondrial lysate was denatured in Tricine sample buffer (Biorad, Veenendaal, The Netherlands) and separated on a 10% SDS-PAGE Tris-Tricine gel for scanning of in-gel fluorescence emission and blotting on nitrocellulose.

2.3. Antibodies and ECL detection

Immunostaining was performed using primary antibodies against ND1 (a gift from Dr. A. Lombès, Inserm U975, Paris, France), the CII 70-kDa subunit (SDHA; Invitrogen) and EGFP (a gift from Dr. F.J. van Kuppeveld, Medical Microbiology, RUNMC, Nijmegen, The Netherlands) in combination with horseradish peroxidase-conjugated secondary antibodies (anti-rabbit or anti-mouse). Signals were detected by ECL (Pierce, Rockford, USA).

2.4. FRAP analysis

Cells were grown to ~70% confluence in a Wilco© dish (Intracel Ltd., Royston, UK). Prior to imaging, culture medium was replaced by a colorless HEPES–Tris (HT) solution (132 mM NaCl, 4.2 mM KCl, 1 mM CaCl₂, 1 mM MgCl₂, 5.5 mM D-glucose and 10 mM HEPES, pH 7.4). FRAP recordings were performed on a ZEISS LSM510 Meta confocal microscope (Carl Zeiss B.V., Sliedrecht, The Netherlands) at a rate of 10 Hz using a ×63 oil immersion objective (N.A. 1.4; zoom factor of 4; optical section thickness <2 µm) as described before [11]. After selection of a mitochondrion of interest (average length of 3 µm), pre-bleach images were collected at 488 nm light from an argon-ion laser set at 0.1% transmission. Next, part of the mitochondrion, referred to as the FRAP region, was photobleached during 500 ms at 100% transmission. Post-bleach images were recorded at 0.1% transmission (Supplemental Fig. S1). The pre-bleach images were used to calculate the initial fluorescence intensity for a mitochondria-free region ($F_{i,background}$), the FRAP region ($F_{i,FRAPregion}$) and the total mitochondrion ($F_{i,totalmito}$). The same was done for each post-bleach image. Individual fluorescence recovery curves ($F(t)$), corrected for the loss of fluorescence and expressed as a percentage of the initial signal, were obtained using:

$$F(t) = 100 \times \frac{\left(\frac{F(t)_{FRAPregion} - F(t)_{background}}{F(t)_{totalmito} - F(t)_{background}} \right) \times \left(\frac{F_{i,totalmito} - F_{i,background}}{F_{i,FRAPregion} - F_{i,background}} \right)}{(1)} \quad (1)$$

Averaged curves of multiple measurements were fitted by a two-component exponential association model using Eq. (2).

$$F(t) = y_0 + A_1 \left(1 - e^{-t/\tau_{\text{fast}}}\right) + A_2 \left(1 - e^{-t/\tau_{\text{slow}}}\right) \quad (2)$$

Finally, the mobile fraction (F_m) was calculated according to:

$$F_m = \frac{F_{\infty} - F_0}{F_{\text{initial}} - F_0} \quad (3)$$

With F_{initial} being 100% by definition, F_{∞} being the fluorescence value at t_{∞} (calculated from Eq. (2)) and F_0 being the fluorescence value immediately after the bleach pulse (Table 1). In order to test whether induction of protein expression as such affected matrix protein diffusion, we compared the fluorescence recovery between the induced and non-induced GFP cell line. No differences in recovery kinetics were observed (data not shown).

2.5. Image processing, curve fitting and statistics

For image processing and analysis we used LSM 510 Meta software (Zeiss) and Image Pro Plus 5.1 (Media Cybernetics, Bethesda, MD, USA). Non-linear curve fitting (using the Levenberg-Marquardt algorithm) and statistical analysis was performed using Origin Pro 7.5 (Originlabs, Northampton, MA, USA). Values from multiple experiments are expressed as mean \pm SEM (standard error of the mean).

3. Results

3.1. Assembly patterns of fluorescently labeled CI structural and assembly factor proteins after inhibition of mitochondrial translation

The effect of ND-subunit depletion on the assembly pattern of several nDNA-encoded CI subunits and a recently discovered CI

assembly factor was investigated in inducible HEK293 cell lines expressing AcGFP1-tagged versions of these proteins [11,31]. To obtain information about the different functional modules of the complex, we selected NDUFV1 and NDUFS3, predicted to be structural subunits of the dehydrogenase and hydrogenase module, respectively. In addition, we included NDUF2 and NDUFB6, thought to reside in the matrix-protruding and membrane arm, respectively, and the CI assembly factor NDUF4. Four of the five cell lines (NDUFV1, NDUFS3, NDUF2, NDUF4) expressed the tagged subunit under non-induced conditions (leakage) which minimized the risks of overexpression artifacts. An additional advantage is that under leakage conditions the incorporation of tagged proteins is at steady state. Importantly, in previous work we showed that CI-incorporation of AcGFP1-tagged NDUFV1, NDUFS3, NDUF2, NDUFB6 and NDUF4 did not alter CI expression and activity, even when their expression levels were high [10,11,31,41]. In line with these findings, AcGFP1-tagged NDUFS3, NDUF2, NDUFB6 and NDUF4 showed similar assembly patterns as their endogenous counterparts. However, the best proof for their functionality was delivered by AcGFP1-tagged NDUF2 and NDUF4, which could complement CI deficient patient cells containing mutations in their endogenous genes [20,31].

The assembly pattern of the five AcGFP1-tagged proteins was analyzed on native gels of mitochondrial fractions from cells cultured in the absence (–) and presence (+) of the mitochondrial translation blocker chloramphenicol (CAP; Fig. 1A). Labeled holo CI and its subassemblies were visualized by fluorescence scanning of the gel (lanes marked f) and immunostaining with an anti-EGFP antibody on a Western blot of the same gel (lanes marked a). In the absence of CAP, both detection methods revealed the presence of AcGFP1-tagged subunit at the height of holo CI (closed arrow heads) for NDUFV1, NDUFS3, NDUF2. NDUFB6 showed a very dim smear around CI on the fluoroscan, whereas a more distinct band was observed on the Western blot. No signal at the height of holo CI was visible for assembly factor NDUF4. Using antibody detection, distinct bands of lower MW, previously identified as CI assembly intermediates [31,41], were demonstrated for NDUFS3 and NDUF4 (Fig. 1A, open arrowheads 1–6). As reported previously, an additional band just below CI (open arrowhead 6') was observed for NDUF4 [31]. For NDUFV1 and NDUF2, also other (faint) bands of lower MW were seen, whereas NDUFB6 showed a smear below CI, compatible with previous findings [11,40,41].

CAP-treatment greatly reduced the intensity of the signals at the height of holo CI. For NDUFS3, this effect was accompanied by an increase in subcomplexes 2 and 3, whereas subcomplexes 4, 5 and 6 were virtually absent. A similar result was obtained for NDUF4, where both the monomeric form and subcomplex 3 were markedly increased and subcomplexes 4, 5, 6 and 6' were only barely detectable. CAP-treatment diminished the lower MW bands for NDUFV1, NDUF2 and NDUFB6.

Analysis of identical amounts of the same mitochondrial lysates on SDS-PAGE gels revealed lowered expression levels upon CAP-treatment for AcGFP1-tagged NDUFV1, NDUF2 and NDUFB6, whereas the total amount of AcGFP1-tagged NDUFS3 and NDUF4 were hardly altered (Fig. 1B). In addition to the intact fusion proteins also smaller fluorescent breakdown products were observed for NDUFV1, NDUFS3 and NDUF2. Importantly, the expression of tagged subunits in leakage cells is extremely low (for NDUFS3 less than 5% of the total amount of NDUFS3 [10,41]), which makes it unlikely that these breakdown products originate from overexpression. They might rather reflect unavoidable products of protein turnover. Virtually no lower MW-bands were observed in induced NDUFB6–AcGFP1 cells and leakage NDUF4–AcGFP1 cells.

Parallel analysis for CI in-gel activity and mtDNA-encoded ND1 abundance (Fig. 1C, IGA and ND1, respectively) demonstrated that CAP effectively reduced both.

Table 1

Fitting results of the FRAP curves obtained in different HEK293 cell lines in the absence or presence of chloramphenicol (CAP).

Cell line	^a MW	^b N	^c R ²	^d τ_{fast}	^e τ_{slow}	^f F_0	^g F_m
GFP	27.9	38	0.991	0.326 \pm 0.079	1.30 \pm 0.206	11 \pm 1.7	0.96
GFP + CAP	27.9	21	0.991	0.390 \pm 0.140	1.93 \pm 0.228	9.1 \pm 2.0	0.94
GFP ²	55.8	45	0.992	0.485 \pm 0.163	2.40 \pm 0.262	15 \pm 2.4	0.99
GFP ² + CAP	55.8	35	0.998	0.550 \pm 0.097	5.22 \pm 0.819	10 \pm 1.2	0.94
ANT	62.8	116	0.988	0.129 \pm 0.025	8.37 \pm 0.441	21 \pm 1.2	0.63
ANT + CAP	62.8	53	0.984	0.382 \pm 0.084	6.68 \pm 0.462	17 \pm 1.3	0.59
NDUFV1	77.5	68	0.961	0.350 \pm 0.047	3.58 \pm 0.376	29 \pm 1.8	0.53
NDUFV1 + CAP	77.5	26	0.931	0.272 \pm 0.055	1.91 \pm 0.259	22 \pm 3.6	0.73
NDUFS3	55.3	85	0.967	0.382 \pm 0.048	3.72 \pm 0.376	28 \pm 2.0	0.47
NDUFS3 + CAP	55.3	29	0.954	0.632 \pm 0.089	14.2 \pm 5.22	22 \pm 3.0	0.73
NDUF2	39.7	49	0.973	0.244 \pm 0.034	1.75 \pm 0.130	29 \pm 2.6	0.70
NDUF2 + CAP	39.7	31	0.980	0.481 \pm 0.076	2.54 \pm 0.231	21 \pm 2.1	0.81
NDUFB6	44.3	101	0.977	0.162 \pm 0.028	6.89 \pm 0.466	22 \pm 1.8	0.39
NDUFB6 + CAP	44.3	45	0.962	0.259 \pm 0.061	8.81 \pm 0.960	12 \pm 1.6	0.49
NDUF4	50.1	50	0.989	0.569 \pm 0.080	10.7 \pm 1.12	6.8 \pm 1.0	0.54
NDUF4 + CAP	50.1	45	0.989	0.650 \pm 0.178	7.38 \pm 0.619	10 \pm 1.5	0.54

In this table errors (\pm) represent standard error of the mean (SEM).

^a Predicted MW of the protein (kDa), including size of linker (2 kDa) and AcGFP1 (27.9 kDa).

^b Total number of mitochondria analyzed on at least 2 different days.

^c Coefficient of determination, being the proportion of variability in the average FRAP curve that is accounted for by the fit (calculated using Eq. (2)).

^d Time constant of fast FRAP recovery phase in seconds (larger means slower).

^e Time constant of slow FRAP recovery phase in seconds (larger means slower).

^f Starting (minimal) level of fluorescence recovery (% of pre-bleach level).

^g Mobile fraction (calculated using Eq. (3)).

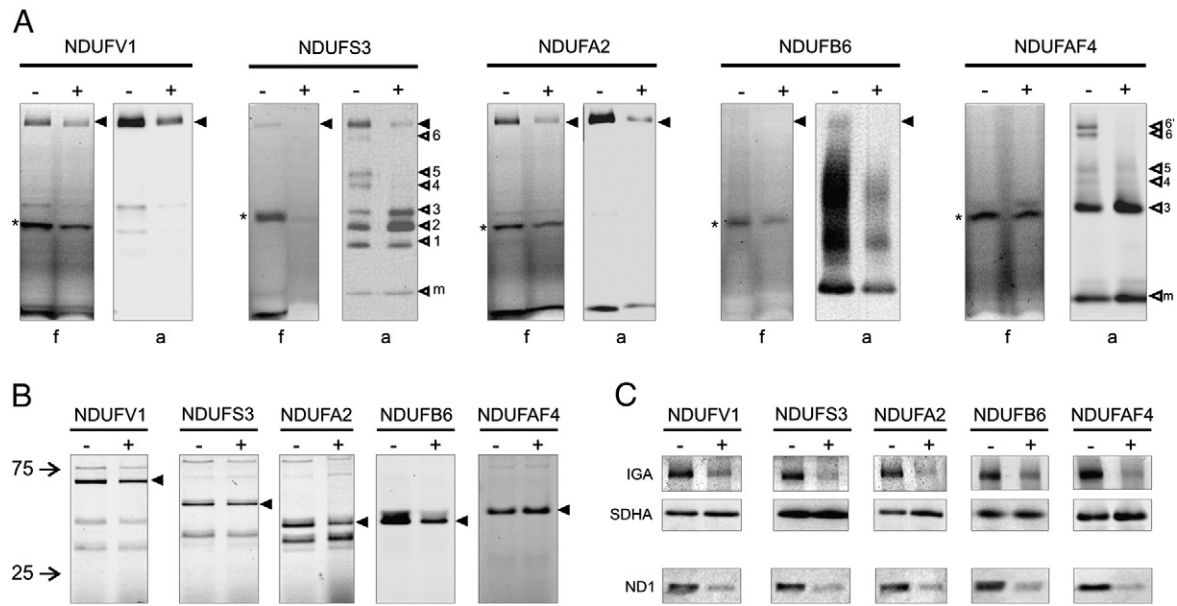


Fig. 1. Effect of CAP on the assembly profile of AcGFP1-tagged CI subunits and assembly factor. Cell lines expressing AcGFP1-tagged NDUFV1, NDUF3, NDUF2, NDUF6 and assembly factor NDUF4 were cultured in the absence (–) or presence (+) of CAP for 3 days. Next, mitochondrial lysates were prepared and subjected to BN- and SDS-PAGE in parallel. (A) Fluorograms of BN-PAGE gels (f) and Western blots of BN-PAGE gels stained with anti-EGFP (a). The position of holo CI is marked with closed arrowheads. Open arrowheads indicate CI assembly intermediates 1–6 and 6' and monomeric protein m. Asterisks indicate specific fluorescent bands also detected in wild type cells (not shown). (B) Fluorograms of SDS-PAGE gels of identical samples shown in A. Closed arrowheads indicate the intact fusion proteins at the expected molecular weight. Height of MW-marker bands (25 and 75 kDa) are indicated by arrows. (C) CI in-gel activity (IGA) measurements on BN-PAGE gels and Western blots of BN-PAGE gels stained with anti-SDHA (SDHA; loading control). Parallel SDS-PAGE Western blots of identical samples stained with anti-ND1 (ND1).

3.2. The mobile fraction of fluorescently labeled CI structural subunits is increased after inhibition of mitochondrial translation

Next, we studied the effect of CAP on the mobility of the nDNA-encoded CI structural subunits and assembly factor NDUF4. To this end, we compared their sub-mitochondrial fluorescence recovery after photobleaching (FRAP) characteristics (Fig. 2A–E) in the absence (closed symbols) and presence (open symbols) of CAP. Recovery kinetics were fitted using a two-component model [11,28] (smooth blue and red curves for (–) and (+) CAP conditions, respectively). On average, the relative amount of mobile molecules (mobile fraction; F_m) for cells cultured in the absence of CAP (Fig. 2F, blue bars and Table 1) ranged between 0.39 (NDUF6) and 0.70 (NDUF2). This indicates that a considerable fraction of tagged subunit (i.e. 61% for NDUF6 and 30% for NDUF2) was immobile in the presence of ND-subunits (Table 1). For all four subunits, CAP treatment increased their F_m (Fig. 2F, red bars and Table 1). In contrast, CAP did not alter the F_m for NDUF4, indicating that its effect on the F_m for CI structural subunits was not due to non-specific effects on protein diffusion in the mitochondrial matrix and/or MIM. To substantiate this conclusion, we analyzed the effect of CAP in three 'control' HEK293 cell lines, conditionally expressing either a mitochondrial matrix-targeted AcGFP1 (cell line designated 'GFP'), a mitochondrial matrix-targeted tandem fusion of AcGFP1 (cell line designated 'GFP²'), or an N-terminal fusion of AcGFP1 to the integral MIM-protein adenine nucleotide translocase 1 (cell line designated 'ANT'). Proper expression of these fusion proteins was demonstrated by SDS-PAGE (Fig. 3A). Fluorescence scanning (lanes indicated f) and anti-EGFP immunostaining (lanes indicated a) revealed specific bands of the expected size in both the absence (–) and presence (+) of CAP. The effectiveness of CAP was demonstrated by the reduction in CI in-gel activity (Fig. 3B, panels indicated IGA) and ND1 expression (Fig. 3C). Recovery curves of GFP, GFP² and ANT cells (Fig. 3D–F), determined in the absence (closed symbols, blue curves) and presence (open symbols, red curves) of CAP, show that blocking mitochondrial translation hardly affected

F_m (Table 1 and Fig. 3G). This supports the above conclusion that ND-subunit depletion specifically increased the mobile fraction of the investigated CI structural subunits.

3.3. The recovery kinetics of fluorescently labeled CI structural subunits is differently altered after inhibition of mitochondrial translation

To further explore the changes in mobility of nDNA-encoded CI subunits upon inhibition of mitochondrial translation we quantified the FRAP kinetics of the mobile proteins. Fitting of the FRAP curves using a two-component model yielded two time constants (Table 1). We previously demonstrated that the rate of the initial fast recovery phase (i.e. t_{fast}) is less informative since it might be affected by small amounts of fluorescent breakdown products [11]. This is substantiated by the fact that the fast component of the FRAP-signal was virtually absent in cells without breakdown products (NDUF6, NDUF4 and ANT cells), reflected by the limited amount of data points constituting their fast phase of the recovery curve (Fig. 2D, E and Fig. 3F). Therefore, we focus on the slower recovery phase (i.e. t_{slow}). Data concerning t_{fast} is presented in Table 1.

Proper comparison of t_{slow} between the different proteins requires that the size of the individual proteins is taken into account [9,11,38]. Therefore, we plotted the t_{slow} values against the molecular weight (MW) of the studied proteins (Fig. 4A, B). To establish this relationship for unconjugated matrix diffusing proteins, a linear fit was calculated through the origin and the coordinates of GFP and GFP² (blue and red lines, respectively). Any t_{slow} value above these lines (e.g. ANT) indicates that fluorescence recovery is slower than expected on the basis of the MW of the protein. This means that the protein is binding to other matrix- or MIM-proteins or to the MIM itself. Here, it should be noted that CAP increased the t_{slow} values of GFP and GFP², whereas it decreased that of ANT. One possible explanation is that CAP alters the ultrastructure and/or density of the mitochondrial matrix as was demonstrated in persons that received CAP-therapy [37]. The underlying cause could be CAP-induced misassembly of F_1/F_0 -ATP synthase

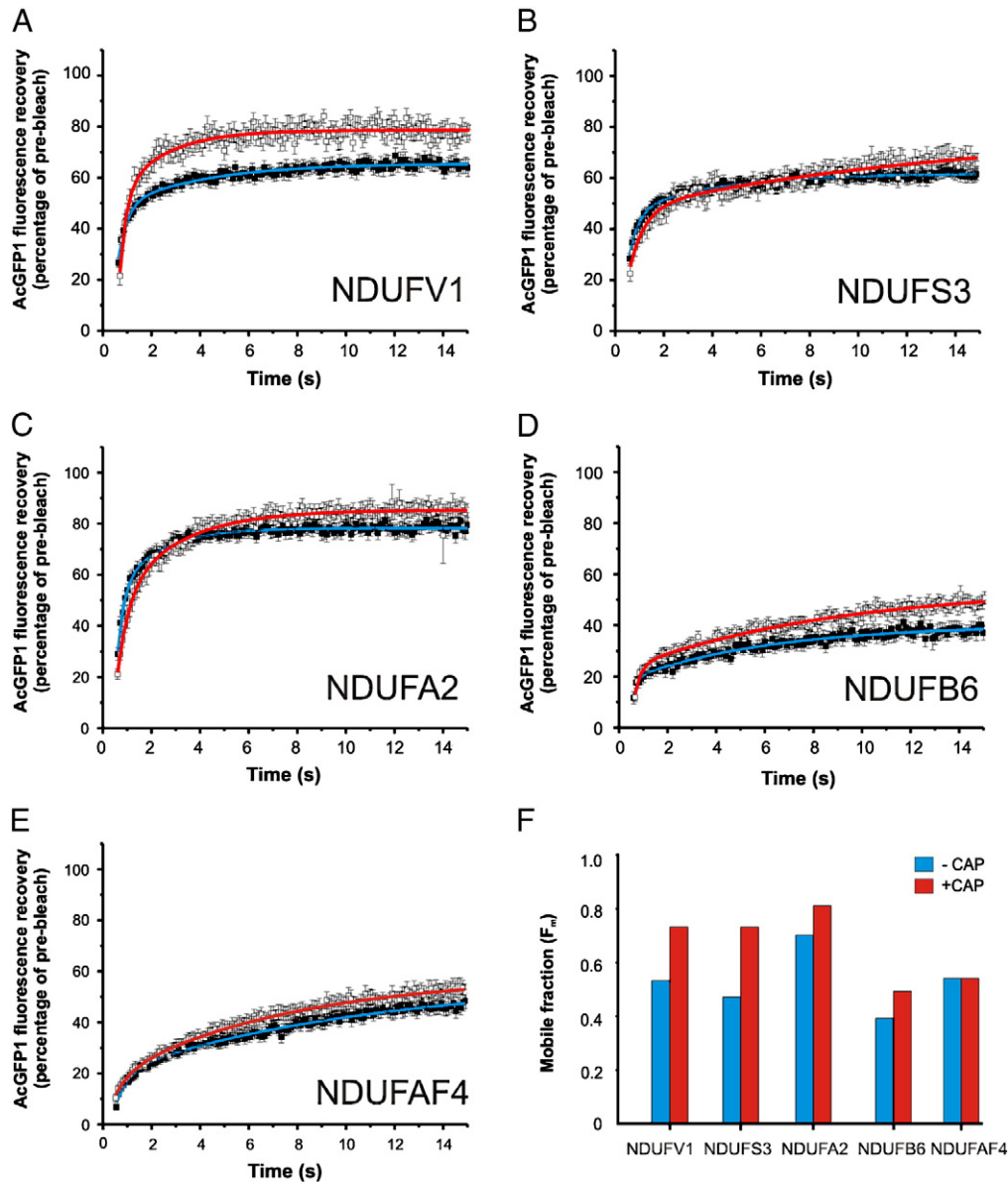


Fig. 2. Effect of CAP on the FRAP kinetics of AcGFP1-tagged CI subunits and assembly factor. Averaged FRAP curves (open and closed symbols) and two-component model fits (blue and red lines) of cell lines cultured in absence (closed symbols, blue lines) or presence (open symbols, red lines) of CAP for 3 days prior to FRAP imaging. (A) NDUFV1, (B) NDUF3, (C) NDUF2, (D) NDUF6 and (E) NDUF4. (F) Relative size of the mobile fraction (F_m) in the different cell lines following culturing in the absence (blue bars) or presence (red bars) of CAP. Mobility values are given in Table 1.

(Supplemental Fig. S2A), the integrity of which is crucial for maintaining cristae morphology [3,18,26]. Recently we have shown that protein diffusion in the mitochondrial matrix is greatly hindered by cristae [9]. We here observed that the number of cristae in CAP-treated cells was reduced when compared to non-treated cells (see Supplemental Fig. S2B/C). This suggests that the slowing effect of CAP on the fluorescence recovery signals of GFP and GFP² is not due to an increase in the number of cristae. This leaves open the possibility that mitochondrial matrix viscosity is increased in CAP-treated cells.

In the absence of CAP (Fig. 4A), the t_{slow} values for NDUF2 and NDUFV1 were located on the line, indicating that they were not bound. On the other hand, those for NDUF3, NDUF6 and NDUF4 were above this line, suggesting slower diffusion due to protein and/or membrane interactions [11]. In CAP-treated cells, we observed an increase in t_{slow} for both GFP and GFP² (Fig. 4B and Table 1). Nevertheless, the relationship between t_{slow} and MW for these proteins

remained linear. Increased t_{slow} values were also observed for NDUF2, which remained virtually on the line, NDUF6, for which the effect was relatively small, and NDUF3, which showed a large decrease in mobility. On the other hand, CAP-treatment decreased t_{slow} for ANT, NDUF4 and NDUFV1. In the case of NDUFV1, the t_{slow} value was clearly located below the line. In fact, this value was similar to that of GFP, suggesting that the mobile fraction represented AcGFP1 rather than AcGFP1-tagged NDUFV1.

In summary, defective mitochondrial translation increased the mobile fraction of all four nDNA-encoded subunits investigated. However, its effect on the mobility of these subunits was large and opposite for NDUFV1 (located in the dehydrogenase module) and NDUF3 (located in the hydrogenase module), relatively small for NDUF6 (located in the membrane module) and virtually absent for NDUF2 (of so far undefined localization). Regarding NDUF4 (a CI assembly factor), CAP-induced ND-subunit depletion did not alter the mobile fraction, while it increased its mobility.

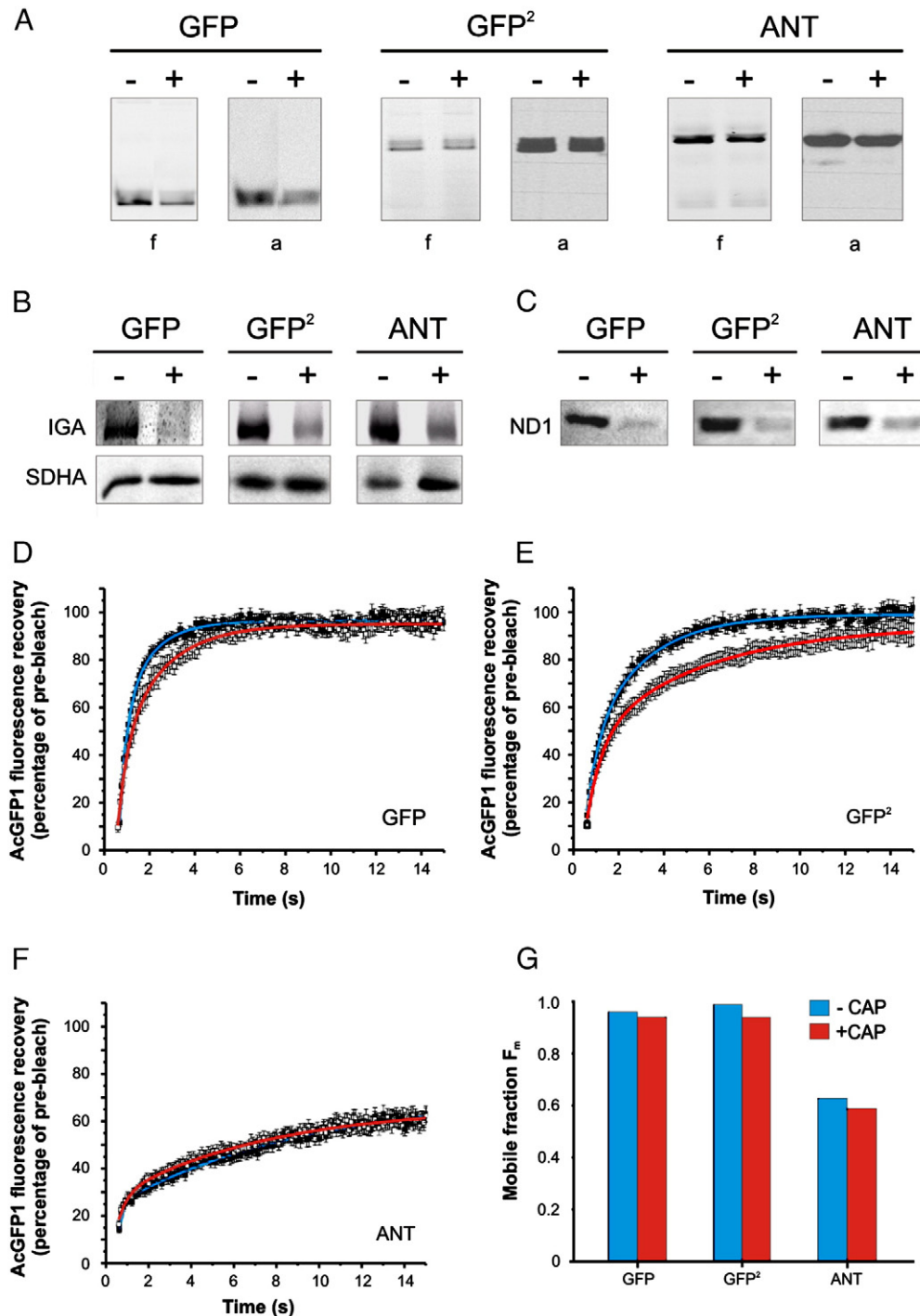


Fig. 3. Effect of CAP on the FRAP kinetics of matrix-soluble and MIM-bound proteins. Cell lines expressing either matrix-targeted AcGFP1 (GFP), matrix-targeted tandem version of AcGFP1 (GFP²) or ANT1-linked AcGFP1 (ANT) were cultured in absence (–) or presence (+) of CAP and processed for BN- and SDS-PAGE as described in the legend to Fig. 1. (A) Fluorograms of SDS-PAGE gels (f) and Western blots of SDS-PAGE gels stained with anti-EGFP (a). (B) CI in-gel activity (IGA) measurements on BN-PAGE gels and anti-SDHA Western blots of BN-PAGE gels (SDHA; loading control). (C) Anti-ND1 Western blots of SDS-PAGE gels (ND1). (D–G) Averaged FRAP curves (open and closed symbols) and two-component model fits (blue and red lines) of cell lines cultured in absence (closed symbols, blue lines) or presence (open symbols, red lines) of CAP. (G) Relative size of the mobile fraction (F_m) in the different cell lines following culturing in the absence (blue bars) or presence (red bars) of CAP. Mobility values are given in Table 1.

4. Discussion

The present study uses FRAP analysis to obtain live cell information about the role of mitochondrial translation in the dynamics of individual CI subunits and their functional CI modules. The strategy chosen was to compare the live cell FRAP characteristics of AcGFP1-

tagged versions of CI subunits and a CI assembly factor in the absence and presence of the mitochondrial translation inhibitor chloramphenicol (CAP). The effectiveness of the CAP-treatment was confirmed by blue native analysis of mitochondrial lysates, showing a marked decrease in the amount of holo CI but not its complete disappearance. Consistent with this finding, FRAP analysis revealed that

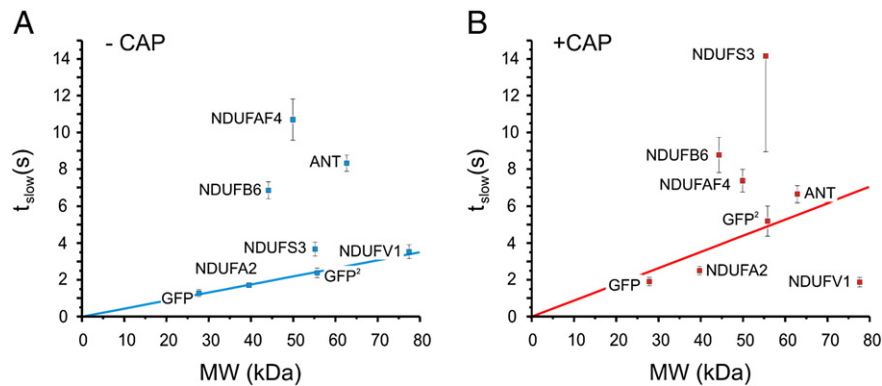


Fig. 4. Effect of CAP on the mobility of the fusion protein as a function of its molecular weight. The kinetics of the recovery phase of the mobile fraction was quantified by fitting to a two-component model, yielding a t_{fast} and a t_{slow} . Because previous work revealed that t_{fast} was little informative [11] we here focus on t_{slow} . (A) Plot of average t_{slow} (mean \pm SEM) versus MW in untreated cells. As reported before [11], the values for GFP and GFP² are on a line through the origin (blue line). (B) Plot of average t_{slow} (mean \pm SEM) versus MW in CAP-treated cells. The values for GFP and GFP² are on a line through the origin (red line). The obtained R values of the fit are 1 ± 0.09 (–CAP) and 1 ± 0.61 (+CAP).

CAP notably decreased the immobile fraction of the four AcGFP1-tagged CI subunits but did not nullify this fraction. The parallel decrease in amount of holo CI and relative size of the immobile fraction, strongly suggests that in the living cell the mobility of the holo complex is very low. This is in agreement with the idea that CI constitutes part of respiratory supercomplexes [4,33,45] and the observation that fluorescently labeled CI shows localized (immobile) patches that do not redistribute over mitochondrial filaments by mitochondrial fusion and fission [5].

4.1. Dynamics of NDUFV1 and the dehydrogenase module

Under normal conditions, 53% of NDUFV1–AcGFP1 is present in the mobile fraction. Our data show that this fraction consists entirely of monomeric NDUFV1–AcGFP1. This conclusion is based on the fact that the mobility of this fraction is exactly as predicted on the basis of its molecular weight. Regarding the GFP-positive subcomplex seen on a BN-gel, this means that it is most probably a MIM-bound intermediate. One important implication of our findings is that under normal conditions the dehydrogenase module exists, if at all, in the membrane-bound form. This strongly suggests that the dehydrogenase module is assembled in a subunit-by-subunit manner on top of a MIM-bound CI intermediate. Keeping this in mind, the picture emerges that the dehydrogenase module is a highly dynamic part of CI that is assembled and disassembled depending on cellular needs. In this context, it would be of interest to assess the effect of changes in metabolic state on the size of the mobile fraction of NDUFV1–AcGFP1.

Intriguingly, CAP-treatment significantly increased the mobility of the mobile fraction of NDUFV1–AcGFP1 to the same value as observed with AcGFP1 alone. This result clearly demonstrates that in CAP-treated cells, in sharp contrast to untreated cells, virtually all unbound NDUFV1–AcGFP1 is removed from the mitochondrial matrix. In other words, this means that either all NDUFV1–AcGFP1 that is left in the mitochondrial matrix is broken down or bound to an immobile (sub)complex. The fact that CAP-treatment does not exert the same effect on the tandem fusion of AcGFP1 strongly suggests that NDUFV1 itself is degraded by a mechanism that leaves its fusion partner AcGFP1 intact. How to explain the decreased amount of unbound NDUFV1–AcGFP1 in the mitochondrial matrix? A possible explanation is that under normal conditions CI-bound NDUFV1 is continuously exchanged for unbound NDUFV1, possibly protecting this subunit from being captured by the machinery that causes its degradation. *In vitro* evidence for such an exchange mechanism has been provided recently [22]. This explanation would be compatible with the above idea of a subunit-by-subunit assembly

of the dehydrogenase module on top of a MIM-bound CI intermediate. Maintenance of this putative intermediate would then require the continuous formation of mtDNA-encoded (ND) subunits so that it will gradually disappear upon inhibition of mitochondrial translation. An alternative explanation is that CAP-treatment might lead to the activation of processes that degrade unbound subunits such as NDUFV1. One possibility might be the increased production of superoxide, which was found to occur (unpublished data) in cultured skin fibroblasts of a patient with a mutation in the mitochondrial translation elongation factor EFTs [35]. Since NDUFV1 contains the NADH binding site, FMN and the N3 iron sulfur cluster [14,19,32], the possibility exists that it takes up electrons and converts these into superoxide and its derived reactive oxygen species (ROS), factors that may contribute to its instability. Moreover, the presence of an iron sulfur cluster may increase its susceptibility for ROS produced by the Fenton reaction.

4.2. Dynamics of NDUF2, a hitherto undefined peripheral arm subunit

The NDUF2 subunit is a paralogue of the mitochondrial ribosomal proteins L43 and S25, suggesting that it may play a role in mitochondrial translation [17]. Under normal conditions, 70% of NDUF2–AcGFP1 is present in the unbound form. In this respect, NDUF2 behaves similar to NDUFV1. CAP-treatment increased its mobile fraction to 81% but, unfortunately, t_{slow} vs. molecular weight analysis did not allow drawing any firm conclusion regarding the effect of this treatment on the intactness of the fusion protein. Most probably, part of it is present in the intact form, whereas the remainder is degraded to AcGFP1. Because mutations in NDUF2 lead to CI deficiency [20], paralleled by a marked decrease in the amount of holo CI, this subunit likely plays a crucial role in CI maintenance and/or stabilization. Why such a role is accompanied with the presence of excess unbound subunit is presently unclear. As for NDUFV1, we speculate that NDUF2 is involved in the regulation of CI activity through the control of its assembly status.

4.3. Dynamics of NDUF3 and the hydrogenase module

Under normal conditions, about 50% of NDUF3–AcGFP1 is present in the immobile fraction proposed before to consist of holo CI and several MIM-bound subcomplexes [11]. The remainder is present in a mobile fraction characterized by a relatively slow mobility. Previous work suggested that this latter fraction likely comprises a matrix-soluble assembly of ~100 kDa consisting of NDUF3–AcGFP1 and several associated proteins [11]. The present study shows that CAP-treatment increased the size of the mobile fraction and, at the

same time, decreased its mobility. First of all, this result demonstrates that NDUF3–AcGFP1, in sharp contrast to NDUFV1–AcGFP1, is preserved in relatively slowly mobile subcomplexes. Another important finding is that CAP-treatment did not result in the formation of new CI subcomplex species but rather changed the relative amounts of already existing subcomplexes as was revealed by blue native gel analysis. In more detail, the latter technique revealed that CAP-treatment decreased the amount of holo CI and its subcomplexes 4, 5, 6 and, to a lesser extent, 1, whereas it increased the amount of subcomplexes 2 and 3 (see also [31,41]). Previous work suggested that subcomplex 1 is matrix-soluble, whereas subcomplexes 2 and 3 are relatively loosely membrane-bound and subcomplexes 4, 5 and 6 are relatively tightly membrane-bound [11]. Taken together, these and the present findings indicate that the CAP-induced increase of the mobile fraction of NDUF3–AcGFP1 reflects the disappearance of holo CI and its subcomplexes 4, 5 and 6, whereas the CAP-induced decrease in mobility of this fraction reflects the decrease in soluble subcomplex 1 and the increase in subcomplexes 2 and 3. This, then, indicates that the latter two complexes are slowly mobile. According to the present concept of CI assembly, these latter two subcomplexes might provide a scaffold for the coordinated translation and incorporation of ND-subunits assisted by CI assembly factors NDUF4 and NDUF4 [31]. After CAP treatment, NDUF4 exists as a MIM-bound monomer and is part of subcomplex 3, but not of subcomplex 2 (also see discussion below). The t_{slow} of NDUF4 after CAP treatment is smaller than the respective t_{slow} of NDUF3. Given the fact that t_{slow} in NDUF3 cells reflects the mobility and kinetics of a mixed population of assemblies, matrix-soluble monomers and possibly breakdown products, these NDUF4 data strongly suggest that subcomplex 2 is much less mobile than subcomplex 3. NDUF3 is considered to be part of the hydrogenase module and the present data suggest that this module, in contrast to the dehydrogenase module, is relatively stable in the absence of mtDNA-encoded subunits. Similar conclusions regarding the stability of CI subunits were drawn from *in vitro* analysis of cells lacking mitochondrial DNA or in which mitochondrial translation was blocked, showing that the amount of some subunits was dramatically decreased, whereas other subunits remained readily detectable [3,29,40,46].

4.4. Dynamics of NDUF6, a component of the membrane arm

On a blue native gel, endogenous and AcGFP1-tagged NDUF6 yields a smear that spreads from holo CI to relatively small subcomplexes [11,40,41]. NDUF6 is an integral membrane protein, so the most likely explanation for this observation is that it forms an early component in the subunit-by-subunit assembly of a relatively large module, probably the membrane arm of the holo complex. Under normal conditions a relatively large part of NDUF6–AcGFP1 (61%) is present in the immobile fraction, suggesting that the vast majority of subcomplexes is virtually immobile. The remainder displays a relatively slow mobility, which likely reflects its composition of a mixture of more or less mobile MIM-bound intermediates. Upon CAP-treatment, both the relative size of the immobile fraction and the mobility of the mobile fraction slightly decreased, suggesting that NDUF6–AcGFP1 containing subcomplexes are relatively inert to inhibition of mitochondrial translation. This, then, means that these subcomplexes predominantly consist of nDNA-encoded subunits, which is in line with our model in which NDUF6 subcomplexes join with mtDNA-encoded subunits in a relatively late stage of assembly to form the mature membrane arm of the complex [41].

4.5. Dynamics of the assembly factor NDUF4

Based on blue native analysis, the CI assembly factor NDUF4 has been proposed to link an early assembly intermediate with the MIM for subsequent joining of mtDNA-encoded subunits [31]. Under

normal conditions, 46% of NDUF4–AcGFP1 is present in the immobile fraction, whereas the remainder is present in a mobile fraction of which the mobility was slower than expected on the basis of the molecular weight of the fusion protein. CAP-treatment did not alter the size of the immobile fraction, whereas it increased the mobility of the mobile fraction. Blue native gel analysis revealed that these effects of CAP were paralleled by the virtual disappearance of the subcomplexes 4, 5, 6 and 6' and the increase in subcomplex 3 and the monomeric form of the fusion protein. Based on previous work showing that subcomplexes 4, 5 and 6 are relatively tightly membrane-bound [11] and the conclusion of this study that subcomplex 3 is slowly mobile, these changes very well explain the relative increase in mobility of the mobile fraction. The mobility of AcGFP1–NDUF4 is significantly lower than that of ANT in both the absence and presence of CAP. Most probably the (sub)complexes that contain NDUF4 are larger, and/or more restricted in diffusion by MIM-microdomains. Together, these results are compatible with NDUF4 binding to a slowly mobile subcomplex 3 that lacks mtDNA-encoded subunits but does contain NDUF3 after which it remains associated with the growing complex until shortly before completion of the holo complex. This last step appears to involve, probably among others, the binding of NDUFV1 and NDUF2, which were not detected in the NDUF3/NDUF4 containing subcomplexes.

Fig. 5 depicts our current model of CI assembly. In this model it is assumed that assembly starts with NDUF3 and a few other nDNA-encoded subunits that form subcomplexes of the hydrogenase module, of which subcomplex 3 is an important one since it binds NDUF4 [31]. This binding of NDUF4 turns subcomplex 3 into a proper scaffold for incorporation of mtDNA-encoded (ND) subunits [31]. Subsequent fusion of other preassembled subcomplexes and subunits results eventually in a mature CI. CAP-treatment preserves NDUF3 in subcomplexes 2 and 3, where it is protected against

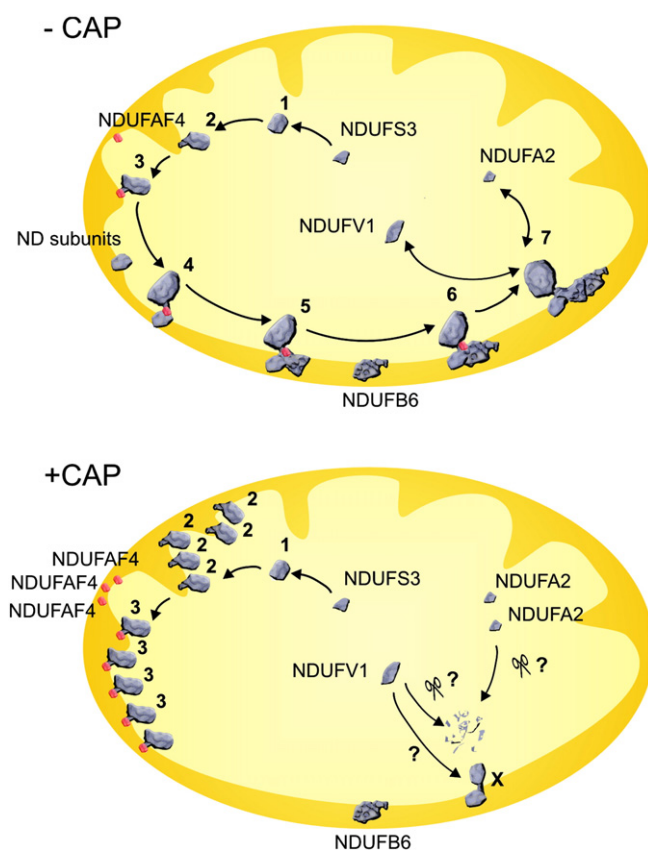


Fig. 5. Schematic presentation of CI assembly (A) under normal conditions and (B) after inhibition of mitochondrial translation (see Discussion for details).

degradation. The latter is not the case for NDUFV1 which is removed from the mitochondrial matrix by either increased breakdown (which might also be the case for NDUFA2), or binding to immobile subcomplexes (indicated X).

In conclusion, our FRAP approach provided the first explorative data of CI subunit dynamics under normal and disturbed assembly conditions in living cells. In the near future this could serve as a new tool to obtain insight into CI assembly defects in live patients cells.

Supplementary materials related to this article can be found online at [doi:10.1016/j.bbabbio.2011.09.013](https://doi.org/10.1016/j.bbabbio.2011.09.013).

Conflict of interest statement

The authors state that there is no conflict of interest.

Acknowledgments

We are grateful to Ing. M. Wijers (Department of Cell Biology, NCMLS) for performing electron microscopy analysis, Dr. A. Lombès (Inserm U975, Paris, France) for providing the anti-ND1 antibody and Dr. F.J. van Kuppeveld (Medical Microbiology, RUNMC, Nijmegen, The Netherlands) for providing the anti-EGFP antibody. This work was supported by a grant of the Radboud University Nijmegen Medical Centre (RUNMC) to WJHK and LGJN, equipment grants of ZON (Netherlands Organization for Health Research and Development, no: 903-46-176), NWO (Netherlands Organization for Scientific Research, no: 911-02-008) and by the CSBR (Centres for Systems Biology Research) initiative from the Nederlandse organisatie voor Wetenschappelijk Onderzoek (NWO, Netherlands Organisation for Scientific Research, grant: #CSBR09/013V).

References

- [1] A.C. Adam, C. Bornhove, H. Prokisch, W. Neupert, K. Hell, The Nfs1 interacting protein Isd11 has an essential role in Fe/S cluster biogenesis in mitochondria, *EMBO J.* 25 (2006) 174–183.
- [2] H. Antonicka, I. Ogilvie, T. Taivassalo, R.P. Anitori, R.G. Haller, J. Vissing, N.G. Kennaway, E.A. Shoubridge, Identification and characterization of a common set of complex I assembly intermediates in mitochondria from patients with complex I deficiency, *J. Biol. Chem.* 278 (2003) 43081–43088.
- [3] I. Bourges, C. Ramus, C.B. Mousson de, R. Beugnot, C. Remacle, P. Cardol, G. Hofhaus, J. P. Issartel, Structural organization of mitochondrial human complex I: role of the ND4 and ND5 mitochondria-encoded subunits and interaction with prohibitin, *Biochem. J.* 383 (2004) 491–499.
- [4] J.B. Bultema, H.P. Braun, E.J. Boekema, R. Kouril, Megacomplex organization of the oxidative phosphorylation system by structural analysis of respiratory supercomplexes from potato, *Biochim. Biophys. Acta* 1787 (2009) 60–67.
- [5] K.B. Busch, J. Bereiter-Hahn, I. Wittig, H. Schagger, M. Jendrach, Mitochondrial dynamics generate equal distribution but patchwork localization of respiratory Complex I, *Mol. Membr. Biol.* 23 (2006) 509–520.
- [6] M.A. Calvaruso, J. Smeitink, L. Nijtmans, Electrophoresis techniques to investigate defects in oxidative phosphorylation, *Methods* 46 (2008) 281–287.
- [7] S. Carilla-Latorre, M.E. Gallardo, S.J. Annesley, J. Calvo-Garrido, O. Grana, S.L. Accari, P.K. Smith, A. Valencia, R. Garesse, P.R. Fisher, R. Escalante, MidA is a putative methyltransferase that is required for mitochondrial complex I function, *J. Cell Sci.* 123 (2010) 1674–1683.
- [8] M.J. Coenen, H. Antonicka, C. Ugalde, F. Sasarman, R. Rossi, J.G. Heister, R.F. Newbold, F.J. Trijbels, L.P. van den Heuvel, E.A. Shoubridge, J.A. Smeitink, Mutant mitochondrial elongation factor G1 and combined oxidative phosphorylation deficiency, *N. Engl. J. Med.* 351 (2004) 2080–2086.
- [9] C.E. Dieteren, S.C. Gielen, L.G. Nijtmans, J.A. Smeitink, H.G. Swarts, R. Brock, P.H. Willems, W.J. Koopman, Solute diffusion is hindered in the mitochondrial matrix, *Proc. Natl. Acad. Sci. U. S. A.* 108 (2011) 8657–8662.
- [10] C.E. Dieteren, W.J. Koopman, L.G. Nijtmans, Chapter 7 Tracing human mitochondrial complex I assembly by use of GFP-tagged subunits, *Methods Enzymol.* 456 (133–51) (2009) 133–151.
- [11] C.E. Dieteren, P.H. Willems, R.O. Vogel, H.G. Swarts, J. Fransen, R. Roepman, G. Crienien, J.A. Smeitink, L.G. Nijtmans, W.J. Koopman, Subunits of mitochondrial complex I exist as part of matrix- and membrane-associated subcomplexes in living cells, *J. Biol. Chem.* 283 (2008) 34753–34761.
- [12] C.J. Dunning, M. McKenzie, C. Sugiana, M. Lazarou, J. Silke, A. Connelly, J.M. Fletcher, D.M. Kirby, D.R. Thorburn, M.T. Ryan, Human CIA30 is involved in the early assembly of mitochondrial complex I and mutations in its gene cause disease, *EMBO J.* 26 (2007) 3227–3237.
- [13] E. Fassone, A.J. Duncan, J.W. Taanman, A.T. Pagnamenta, M.I. Sadowski, T. Holand, W. Qasim, P. Rutland, S.E. Calvo, V.K. Mootha, M. Bitner-Glindzicz, S. Rahman, FOXRED1, encoding an FAD-dependent oxidoreductase complex-I-specific molecular chaperone, is mutated in infantile-onset mitochondrial encephalopathy, *Hum. Mol. Genet.* 19 (2010) 4837–4847.
- [14] M. Finel, J.M. Skehel, S.P. Albracht, I.M. Fearnley, J.E. Walker, Resolution of NADH: ubiquinone oxidoreductase from bovine heart mitochondria into two subcomplexes, one of which contains the redox centers of the enzyme, *Biochemistry* 31 (1992) 11425–11434.
- [15] T. Friedrich, Complex I: a chimaera of a redox and conformation-driven proton pump? *J. Bioenerg. Biomembr.* 33 (2001) 169–177.
- [16] T. Friedrich, D. Scheide, The respiratory complex I of bacteria, archaea and eukarya and its module common with membrane-bound multisubunit hydrogenases, *FEBS Lett.* 479 (2000) 1–5.
- [17] T. Gabaldon, D. Rainey, M.A. Huynen, Tracing the evolution of a large protein complex in the eukaryotes, NADH:ubiquinone oxidoreductase (Complex I), *J. Mol. Biol.* 348 (2005) 857–870.
- [18] P.D. Gavin, M. Prescott, S.E. Luff, R.J. Devenish, Cross-linking ATP synthase complexes in vivo eliminates mitochondrial cristae, *J. Cell Sci.* 117 (2004) 2333–2343.
- [19] J. Hirst, J. Carroll, I.M. Fearnley, R.J. Shannon, J.E. Walker, The nuclear encoded subunits of complex I from bovine heart mitochondria, *Biochim. Biophys. Acta* 1604 (2003) 135–150.
- [20] S.J. Hoefs, C.E. Dieteren, F. Distelmaier, R.J. Janssen, A. Epplen, H.G. Swarts, M. Forkink, R.J. Rodenburg, L.G. Nijtmans, P.H. Willems, J.A. Smeitink, L.P. van den Heuvel, NDUFA2 complex I mutation leads to Leigh disease, *Am. J. Hum. Genet.* 82 (2008) 1306–1315.
- [21] W.J. Koopman, L.G. Nijtmans, C.E. Dieteren, P. Roestenberg, F. Valsecchi, J.A. Smeitink, P.H. Willems, Mammalian mitochondrial complex I: biogenesis, regulation, and reactive oxygen species generation, *Antioxid. Redox Signal.* 12 (2010) 1431–1470.
- [22] M. Lazarou, M. McKenzie, A. Ohtake, D.R. Thorburn, M.T. Ryan, Analysis of the assembly profiles for mitochondrial- and nuclear-DNA-encoded subunits into complex I, *Mol. Cell. Biol.* 27 (2007) 4228–4237.
- [23] J. Nouns, L. Nijtmans, S.M. Houten, M. van den Brand, M. Huynen, H. Venselaar, S. Hoefs, J. Gloerich, J. Kronick, T. Hutchin, P. Willems, R. Rodenburg, R. Wanders, L. van den Heuvel, J. Smeitink, R.O. Vogel, Acyl-CoA dehydrogenase 9 is required for the biogenesis of oxidative phosphorylation complex I, *Cell Metab.* 12 (2010) 283–294.
- [24] I. Ogilvie, N.G. Kennaway, E.A. Shoubridge, A molecular chaperone for mitochondrial complex I assembly is mutated in a progressive encephalopathy, *J. Clin. Invest.* 115 (2005) 2784–2792.
- [25] D.J. Pagliarini, S.E. Calvo, B. Chang, S.A. Sheth, S.B. Vafai, S.E. Ong, G.A. Walford, C. Sugiana, A. Boneh, W.K. Chen, D.E. Hill, M. Vidal, J.G. Evans, D.R. Thorburn, S.A. Carr, V.K. Mootha, A mitochondrial protein compendium elucidates complex I disease biology, *Cell* 134 (2008) 112–123.
- [26] P. Paumard, J. Vaillier, B. Coulary, J. Schaeffer, V. Soubannier, D.M. Mueller, D. Brethes, J.P. di Rago, J. Velours, The ATP synthase is involved in generating mitochondrial cristae morphology, *EMBO J.* 21 (2002) 221–230.
- [27] E. Perales-Clemente, E. Fernandez-Vizarra, R. Acin-Perez, N. Movilla, M.P. Bayona-Bafaluy, R. Moreno-Loshuertos, A. Perez-Martos, P. Fernandez-Silva, J.A. Enriquez, Five entry points of the mitochondrially encoded subunits in Mammalian complex I assembly, *Mol. Cell. Biol.* 30 (2010) 3038–3047.
- [28] D. Picard, E. Suslova, P.A. Briand, 2-color photobleaching experiments reveal distinct intracellular dynamics of two components of the Hsp90 complex, *Exp. Cell Res.* 312 (2006) 3949–3958.
- [29] P. Potluri, N. Yadava, I.E. Scheffler, The role of the ESSS protein in the assembly of a functional and stable mammalian mitochondrial complex I (NADH-ubiquinone oxidoreductase), *Eur. J. Biochem.* 271 (2004) 3265–3273.
- [30] A. Saada, S. Edvardson, M. Rapoport, A. Shaag, K. Amry, C. Miller, H. Lorberbaum-Galski, O. Elpeleg, C6ORF66 is an assembly factor of mitochondrial complex I, *Am. J. Hum. Genet.* 82 (2008) 32–38.
- [31] A. Saada, R.O. Vogel, S.J. Hoefs, M.A. van den Brand, H.J. Wessels, P.H. Willems, H. Venselaar, A. Shaag, F. Barghuti, O. Reish, M. Shohat, M.A. Huynen, J.A. Smeitink, L. P. van den Heuvel, L.G. Nijtmans, Mutations in NDUFAF4 (C3ORF60), encoding an NDUFAF4 (C6ORF66)-interacting complex I assembly protein, cause fatal neonatal mitochondrial disease, *Am. J. Hum. Genet.* 84 (2009) 718–727.
- [32] L.A. Sazanov, P. Hinchliffe, Structure of the hydrophilic domain of respiratory complex I from *Thermus thermophilus*, *Science* 311 (2006) 1430–1436.
- [33] H. Schagger, Respiratory chain supercomplexes of mitochondria and bacteria, *Biochim. Biophys. Acta* 1555 (2002) 154–159.
- [34] A.D. Sheftel, O. Stehling, A.J. Pierik, D.J. Netz, S. Kerscher, H.P. Elsasser, I. Wittig, J. Balk, U. Brandt, R. Lill, Human Ind1, an iron-sulfur cluster assembly factor for respiratory complex I, *Mol. Cell. Biol.* 29 (2009) 6059–6073.
- [35] J.A. Smeitink, O. Elpeleg, H. Antonicka, H. Diepstra, A. Saada, P. Smits, F. Sasarman, G. Vriend, J. Jacob-Hirsch, A. Shaag, G. Rechavi, B. Welling, J. Horst, R.J. Rodenburg, H.B. Van Den, E.A. Shoubridge, Distinct clinical phenotypes associated with a mutation in the mitochondrial translation elongation factor EFTs, *Am. J. Hum. Genet.* 79 (2006) 869–877.
- [36] J.A. Smeitink, M. Zeviani, D.M. Turnbull, H.T. Jacobs, Mitochondrial medicine: a metabolic perspective on the pathology of oxidative phosphorylation disorders, *Cell Metab.* 3 (2006) 9–13.
- [37] U. Smith, D.S. Smith, A.A. Yunis, Chloramphenicol-related changes in mitochondrial ultrastructure, *J. Cell Sci.* 7 (1970) 501–521.
- [38] B.L. Sprague, J.G. McNally, FRAP analysis of binding: proper and fitting, *Trends Cell Biol.* 15 (2005) 84–91.
- [39] C. Sugiana, D.J. Pagliarini, M. McKenzie, D.M. Kirby, R. Salemi, K.K. bu-Amro, H.H. Dahl, W.M. Hutchison, K.A. Vascotto, S.M. Smith, R.F. Newbold, J. Christodoulou, S.

- Calvo, V.K. Mootha, M.T. Ryan, D.R. Thorburn, Mutation of C20orf7 disrupts complex I assembly and causes lethal neonatal mitochondrial disease, *Am. J. Hum. Genet.* 83 (2008) 468–478.
- [40] C. Ugalde, R. Vogel, R. Huijbens, H.B. Van Den, J. Smeitink, L. Nijtmans, Human mitochondrial complex I assembles through the combination of evolutionary conserved modules: a framework to interpret complex I deficiencies, *Hum. Mol. Genet.* 13 (2004) 2461–2472.
- [41] R.O. Vogel, C.E. Dieteren, L.P. van den Heuvel, P.H. Willems, J.A. Smeitink, W.J. Koopman, L.G. Nijtmans, Identification of mitochondrial complex I assembly intermediates by tracing tagged NDUFS3 demonstrates the entry point of mitochondrial subunits, *J. Biol. Chem.* 282 (2007) 7582–7590.
- [42] R.O. Vogel, R.J. Janssen, C. Ugalde, M. Grovenstein, R.J. Huijbens, H.J. Visch, L.P. van den Heuvel, P.H. Willems, M. Zeviani, J.A. Smeitink, L.G. Nijtmans, Human mitochondrial complex I assembly is mediated by NDUFAF1, *FEBS J.* 272 (2005) 5317–5326.
- [43] R.O. Vogel, R.J. Janssen, M.A. van den Brand, C.E. Dieteren, S. Verkaart, W.J. Koopman, P.H. Willems, W. Pluk, L.P. van den Heuvel, J.A. Smeitink, L.G. Nijtmans, Cytosolic signaling protein Ecsit also localizes to mitochondria where it interacts with chaperone NDUFAF1 and functions in complex I assembly, *Genes Dev.* 21 (2007) 615–624.
- [44] R.O. Vogel, J.A. Smeitink, L.G. Nijtmans, Human mitochondrial complex I assembly: a dynamic and versatile process, *Biochim. Biophys. Acta* 1767 (2007) 1215–1227.
- [45] I. Wittig, R. Carrozzo, F.M. Santorelli, H. Schagger, Supercomplexes and subcomplexes of mitochondrial oxidative phosphorylation, *Biochim. Biophys. Acta* 1757 (2006) 1066–1072.
- [46] N. Yadava, T. Houchens, P. Potluri, I.E. Scheffler, Development and characterization of a conditional mitochondrial complex I assembly system, *J. Biol. Chem.* 279 (2004) 12406–12413.